ISSN 1561-8331 (Print)
ISSN 2524-2342 (Online)
УДК 577.112, 577.112.85
https://doi.org/10.29235/1561-8331-2026-62-4-323-332

Поступила в редакцию 11.08.2026
Received 11.08.2026

Y. D. Khyuppenen, A. S. Savich, M. S. Kisel, A. V. Svirid

Institute of Bioorganic Chemistry, National Academy of Sciences of Belarus, Minsk, Belarus

RECOMBINANT PRODUCTION IN *ESCHERICHIA COLI*, FUNCTIONAL ASSESSMENT AND *IN SILICO* INTERACTOME MAPPING OF HUMAN CYP2J2

Abstract. Cytochrome P450 2J2 (CYP2J2) is an epoxygenase expressed in various tissues, including cardiomyocytes, enterocytes, and vascular endothelial cells. This enzyme participates in the metabolism of arachidonic acid and other polyunsaturated fatty acids, and serves as a significant factor in drug metabolism. In this study, a system was developed for obtaining recombinant human CYP2J2 in *Escherichia coli*. The obtained protein was subjected to a two-step purification using affinity chromatography and hydroxyapatite sorbent chromatography. For several active-site ligands, apparent dissociation constants of the complexes (K_d) were determined. For the first time, the AlphaFold Multimer computational approach was applied for the computational screening of potential protein partners of CYP2J2, allowing the identification of a number of proteins involved in the regulation of the ubiquitin-proteasome pathway, signal transduction, and DNA repair.

Keywords: cytochrome P450, CYP2J2, recombinant protein, epoxygenase, protein-protein interactions, AlphaFold, *in silico* screening

For citation. Khyuppenen Y. D., Savich A. S., Kisel M. S., Svirid A. V. Recombinant production in *Escherichia coli*, functional assessment and *in silico* interactome mapping of human CYP2J2. *Vestsi Natsyyanal'nai akademii navuk Belarusi. Seryya khimichnykh navuk = Proceedings of the National Academy of Sciences of Belarus. Chemical Series*, 2026, vol. 62, no. 4, pp. 323–332 (in Russian). https://doi.org/10.29235/1561-8331-2026-62-4-323-332

Е. Д. Хюппенен, А. С. Савич, М. С. Кисель, А. В. Свирид

Институт биоорганической химии НАН Беларуси, Национальная академия наук Беларуси, Минск, Беларусь

ПОЛУЧЕНИЕ РЕКОМБИНАНТНОГО БЕЛКА В КЛЕТКАХ *ESCHERICHIA COLI*, ФУНКЦИОНАЛЬНАЯ ОЦЕНКА И *IN SILICO* КАРТИРОВАНИЕ ИНТЕРАКТОМА CYP2J2 ЧЕЛОВЕКА

Аннотация. Цитохром P450 2J2 (CYP2J2) представляет собой эпоксигеназу, экспрессируемую в различных тканях, включая кардиомиоциты, энтероциты и клетки сосудистого эндотелия. Данный фермент участвует в метаболизме арахидоновой и других полиненасыщенных жирных кислот, а также выполняет роль значимого фактора метаболизма лекарственных препаратов. Разработана система получения рекомбинантного CYP2J2 человека в бактериях *Escherichia coli*. Была применена стратегия по очистке с применением аффинной хроматографии и хроматографии на гидроксиапатитном сорбенте. Для ряда лигандов активного центра определены кажущиеся константы диссоциации комплексов (K_d). Впервые применен вычислительный подход AlphaFold Multimer для идентификации потенциальных белков-партнеров CYP2J2, позволивший выявить ряд белков, вовлеченных в регуляцию убиквитин-протеасомного пути, передачу сигнала и репарацию ДНК.

Ключевые слова: цитохром P450, CYP2J2, рекомбинантный белок, эпоксигеназа, белок-белковые взаимодействия, AlphaFold, *in silico* скрининг

Для цитирования. Получение рекомбинантного белка в клетках *Escherichia coli*, функциональная оценка и *in silico* картирование интерактома CYP2J2 человека / Е. Д. Хюппенен, А. С. Савич, М. С. Кисель, А. В. Свирид // Весці Нацыянальнай акадэміі навук Беларусі. Серыя хімічных навук. – 2026. – Т. 62, № 4. – С. 323–332 https://doi.org/10.29235/1561-8331-2026-62-4-323-332

Introduction. Cytochrome P450 enzymes (CYPs) constitute a superfamily of monooxygenases playing an essential role in the metabolism of endogenous compounds and xenobiotics [1]. Among the diverse families within this superfamily, CYP2 represents a particularly important group of enzymes with distinct tissue-specific distribution patterns and substrate specificities [2]. Members of the CYP2 family are involved in the oxidative metabolism of fatty acids, steroids, eicosanoids, and numerous pharmaceutical agents, thereby influencing physiological homeostasis and pharmacological outcomes [3].

Within the CYP2 family, CYP2J2 stands out as a non-hepatic isoform with a tissue distribution pattern fundamentally different from that of hepatic isoforms of the same family. The highest levels of CYP2J2 expression have been documented in cardiomyocytes, where it serves as the dominant epoxygenase of arachidonic acid, as well as in enterocytes of the small intestine, lung tissue, vascular endothelial cells, adrenal glands, and brain [4, 5]. This unique distribution profile suggests that CYP2J2 plays critical roles in cardiovascular homeostasis, gastrointestinal function and neurovascular regulation.

The principal endogenous function of CYP2J2 is the bioactivation of polyunsaturated fatty acids. Regarding arachidonic acid, the enzyme acts as an epoxygenase generating four regioisomeric epoxyeicosatrienoic acids (EETs): 5,6-, 8,9-, 11,12- and 14,15-EET. In the myocardium, the reaction exhibits high stereoselectivity with the predominant formation of 14(R),15(S)-EET [6, 7]. In addition to arachidonic acid, CYP2J2 demonstrates a high affinity for omega-3 fatty acids: docosahexaenoic acid is metabolized to epoxydocosapentaenoic acids, eicosapentaenoic acid – to epoxyeicosatetraenoic acids, while linoleic acid is converted predominantly to 9,10- and 12,13-epoxyoctadecenoic acids capable of exerting cytotoxic effects at high concentrations [8, 9].

Beyond endogenous substrates, CYP2J2 participates in oxidative metabolism of a wide range of xenobiotics, including antihistamines (terfenadine, astemizole, ebastine), cardiological drugs (amiodarone, dronedarone), tamoxifen, cyclosporin A, nabetasone and various anthelminthic agents (albendazole, fenbendazole) [10, 11]. Of particular clinical significance in this context is the intestinal expression of the enzyme: the metabolism of pharmaceutical agents in enterocytes directly determines their systemic bioavailability upon oral administration.

Despite the well-established biological importance of CYP2J2, systematic investigations of its molecular interactions remain limited. The enzyme operates within complex macromolecular assemblies involving redox partner proteins, yet comprehensive profiling of its interaction network has not been performed. Recent advances in computational structural biology, particularly the development of AlphaFold-Multimer and related approaches, now enable prediction of protein-protein interactions with unprecedented accuracy [12, 13]. These tools open new possibilities for identifying previously unknown protein partners of CYP enzymes and for understanding their functional networks beyond classical monooxygenase activity.

The present study was designed to address several interrelated objectives: (1) the development of the system for production and purification of recombinant human CYP2J2, (2) the characterization of the catalytically competent enzyme fraction and evaluation of its ligand-binding properties through spectrophotometric titration, and (3) the computational prediction of potential protein interaction partners using the AlphaPulldown pipeline based on AlphaFold-Multimer. The combination of experimental and computational approaches employed in this work provides a foundation for future functional studies of the CYP2J2 interaction networks.

Materials and methods. *Materials.* Reagents used in this study included LB, TB and LB-agar media (Conda, Spain); NaCl, KCl, $MgCl_2$, Na_2HPO_4, K_2HPO_4, $MgSO_4$, $CaCl_2$, imidazole (Thermo Fisher Scientific, USA); $ZnSO_4$, $MnCl_2$, $CoCl_2$, Na_2MoO_4, D-arabinose, D-biotin (Sigma, Germany); acrylamide, CHAPS, dithiothreitol (DTT), acetic acid, glycerol, SDS, Tween-20, IPTG, ALA, Coomassie G-250 (Serva, Germany); Tris (Melford, UK); beta-mercaptoethanol (AppliChem, Germany); hydroxyapatite sorbent Bio-Gel HTP (Bio-Rad, USA); TEMED, ampicillin, kanamycin, agarose (Glentham, UK); HRP-conjugated anti-His-tag antibodies (E-AB-20008), chemiluminescence reagent kit (Elabscience, China).

Expression vectors and plasmids. The prokaryotic expression vector pCW-LIC-2J2-cw02 was constructed for production of recombinant CYP2J2 in *E. coli* using a ligase-independent cloning (LIC) system. The vector contains the tac promoter, ampicillin resistance gene, and the CYP2J2 coding sequence (N′-truncated to omit the membrane anchor, C′-6x-histidine tagged). The plasmid was maintained in the collection of the Laboratory of Molecular Diagnostics and Biotechnology, Institute of Bioorganic Chemistry, National Academy of Sciences of Belarus.

Equipment. Protein purification was performed on the ÄKTApurifier 10 medium-pressure chromatography system (GE Healthcare, Sweden). Absorption spectra were recorded on Cary 5000 UV-Vis-NIR (Agilent Technologies, USA) and DeNovix DS-11 spectrophotometers (DeNovix, USA). Bacterial cell cultivation was carried out in a Multitron Pro shaker-incubator (Infors HT, Switzerland). Molecular masses of proteins and peptides were determined by MALDI-TOF mass spectrometry on a Microflex LRF instrument (Bruker Daltonik GmbH, Germany). Cell disruption of *E. coli* was performed using an Emulsiflex C3 homogenizer (Avestin, Canada). SDS-PAGE was carried out using a CLINX XinPRO system (Clinx, China). Bacterial cultures were pelleted using a ScanSpeed 2236R floor centrifuge (Labogene, Denmark), and clarified cell lysates were obtained using an Avanti J-25 centrifuge (Beckman Coulter, USA). Computer modeling was performed on a computing cluster of the Institute of Bioorganic Chemistry, National Academy of Sciences of Belarus (4xNvidia RTX 5090, 7975WX, 256 GB DDR5 RAM).

Methods. Protein expression and purification. Heterologous expression was carried out in *E. coli* BL21(DE3) cells in a volume of 2 L of culture medium. The cells were co-transformed with the

expression plasmid and the pGro12 plasmid carrying the chaperonine genes groEL/ES. These proteins ensure the proper folding of recombinant cytochromes and increase the overall product yield; their expression was induced by the addition of L-arabinose. On the day preceding the experiment, a seed culture was inoculated into LB medium supplemented with ampicillin and kanamycin. The next day, the culture was diluted 100-fold in two 2 L flasks containing the TB medium with the same antibiotics and a trace elements mixture (54 mM $FeCl_3$, 12 mM $ZnCl_2$, 400 μM each of $CoCl_2$, $CuCl_2$, Na_2MoO_4, $MnCl_2$ and Na_2SeO_3). The cultures were grown at 37 °C and 190 rpm until the optical density reached 0.6-0.8 units.

Upon reaching the desired cell density, IPTG was added to the medium for induction of the target gene expression, along with δ-aminolevulinic acid (δ-ALA) as a precursor of the prosthetic group of cytochromes, and L-arabinose for the activation of chaperone expression. After that, the temperature was reduced to 30 °C. Expression was carried out for 48 h for CYP2J2 in accordance with literature data [14].

After expression, the cells were pelleted by centrifugation; the pellet was resuspended in buffer (50 mM potassium phosphate buffer, pH 7.4; 20 % glycerol; 0.3 M NaCl; 0.3 % CHAPS; 1 mM PMSF) at a ratio of 1 : 4. Cell disruption was performed by passing the suspension twice through a high-pressure homogenizer. For the solubilization of membrane proteins, CHAPS was additionally added to the lysate to a final concentration of 1 % and incubated at 4 °C for 1 h with constant stirring. Cell debris was removed by centrifugation at 30 000 g for 1.5 h. The resulting clarified lysate was used for the subsequent affinity chromatography.

For the purification of the recombinant proteins carrying a His-tag, affinity chromatography was performed on a 5 mL HisTrap HP column (Cytiva, USA). Washing was performed sequentially at imidazole concentrations of 30 mM and 50 mM, followed by the application of a linear gradient to separate impurities from the target protein. Elution of the target protein was performed at 500 mM imidazole. Protein yield was monitored spectrophotometrically at 280 nm.

Hydroxyapatite (HA) chromatography was used as the second purification stage. Before applying to HA, the protein was concentrated and diluted with 10 mM Tris-HCl pH 7.4 buffer without imidazole. Elution was performed with a stepwise gradient of potassium phosphate buffer (KPB); the colored band migrated down the column with increasing KPB concentration, and the target protein was collected at 500 mM KPB as brown-colored fractions.

K_d estimation from differential spectrophotometric titration data. For the selected compounds, spectrophotometric titration with sequential ligand addition and the recording of difference spectrum changes was performed. From the saturation curves of the dependence of ΔA on ligand concentration, the dissociation constants (K_d) were calculated [15]:

$$A = A_{\max} \frac{[L]+[E]+K_d - \sqrt{([L]+[E]+K_d)^2 - 4[E][L]}}{2[E]}$$

where A is the spectral response amplitude at the ligand concentration [L]; $A_{\max}$ is the spectral response amplitude when the enzyme is saturated with the ligand; [L] is the current ligand concentration in solution; [E] is the enzyme concentration.

Computational screening of potential protein partners of CYP2J2. To identify putative protein partners of CYP2J2, we performed a systematic *in silico* screening using the AlphaPulldown v2.1.5 pipeline, which leverages the AlphaFold-Multimer v3 architecture to predict binary and multiprotein complexes. As candidate interactors, we compiled a library of human proteins with experimentally annotated expression in physiologically relevant tissues, sourced from the Human Protein Atlas database (https://www.proteinatlas.org). Proteins with documented cytoplasmic, nuclear, membrane-associated, or mitochondrial localizations were included, reflecting the subcellular distribution of CYP2J2 and its known substrates. For each enzyme, approximately 5,000 potential pairwise interactions were computationally evaluated.

Results and discussion. *Protein expression and purification.* The first stage of this work was the preparation of purified recombinant CYP2J2. This task pursued two goals: first, to confirm that the construct encodes functional and a stable protein suitable for further work; and second, to create a reproducible system for enzyme isolation for subsequent ligand testing under *in vitro* conditions.

IMAC is based on the ability of a polyhistidine fragment of the protein to specifically bind to Ni^{2+} ions immobilized on the matrix, allowing the selective retention of the target protein during sample

loading, while most impurities are removed during washing. The necessity of a second chromatographic step was determined by the presence of imidazole in the eluate after the Ni-NTA column: imidazole coordinates the Fe atom of the heme, blocking the active site of the enzyme and making it incompatible with subsequent functional studies. Hydroxyapatite resin mixed-mode binding is well suited for cytochromes P450. In addition, this method is especially robust for these objects: when the sample was applied to the column, a characteristic brown ring was clearly visible forming at the binding site of the heme-containing protein on the resin.

The imidazole removal efficiency was controlled spectrophotometrically: in the absolute absorption spectra, the maximum in the Soret band region shifted from 425 nm to 419 nm, indicating the restoration of the native state of the heme center and the displacement of imidazole from the coordination sphere of iron (Figure 1).

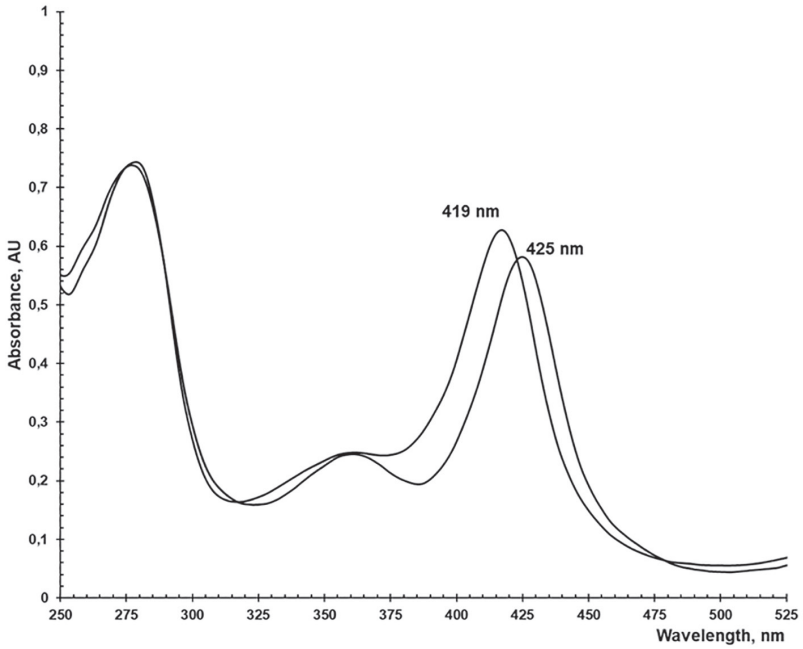


Fig. 1. Absolute absorption spectra of CYP2J2 before and after the imidazole removal

As shown in Figure 2, *a*, MALDI-TOF mass spectrometry confirmed that the experimentally determined molecular mass matches the theoretical value calculated from the amino acid sequence. SDS-PAGE analysis of CYP2J2 (Figure 2, *b*) showed a pronounced band with a molecular mass of approximately 55 kDa, in addition to densitometry analysis that suggests protein preparation purity of > 95 %. Protein identity was confirmed by Western blotting with anti-His-tag antibodies (Figure 2, *c*): a specific signal was detected exclusively at the expected molecular mass level.

The yield of purified CYP2J2 was 21.5 mg/L of culture (~10 g of cells). The purity of the final protein preparations was > 95 % (by SDS-PAGE).

Confirmation of the presence of a catalytically active form in the preparation was performed by CO-difference spectrophotometry. After reduction with sodium dithionite and saturation with carbon monoxide, the CO-difference spectrum of the purified protein revealed a prominent Soret peak at 450 nm, characteristic of the catalytically competent cytochrome P450, with a minor peak at 420 nm corresponding to the inactive P420 form (Figure 3). Analysis of the peaks (corrected by the extinction coefficients for P450 and P420) on the spectrum yielded a P450 : P420 ratio of ~81 : 19, indicating that > 80 % of the spectrally detectable hemoprotein was in the active P450 state. This confirms the successful folding and heme incorporation of the recombinant CYP2J2. Using the extinction coefficient $\varepsilon_{450-490}$ = = 91mM^{-1}cm^{-1} [16], the concentration of functional P450 was calculated accordingly.

Functional activity testing of recombinant protein. To test the functional activity of the obtained preparations, their interaction with compounds known from the literature as ligands of CYP2J2, as well as with a series of potential substrates from the Institute of Bioorganic Chemistry collection, was

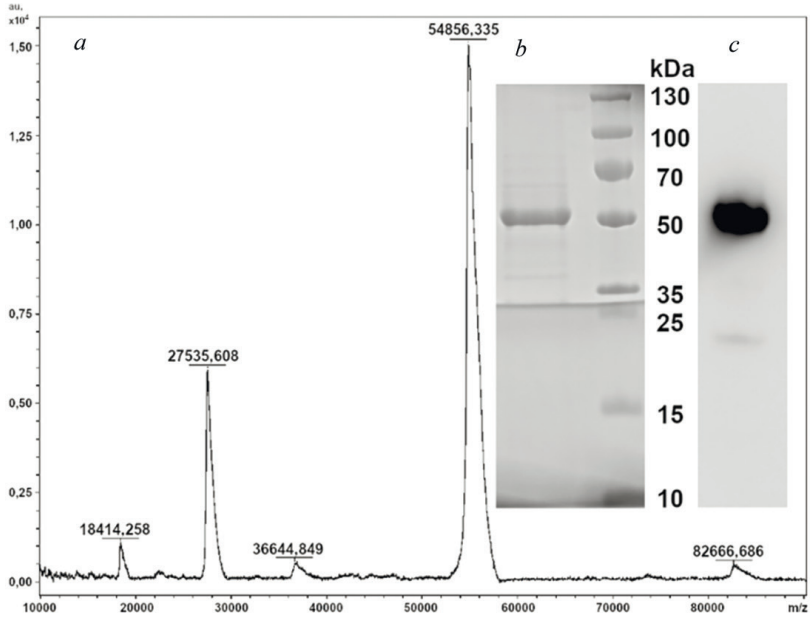


Fig. 2. CYP2J2 physicochemical properties:
a – MALDI-TOF spectrum, *b* – SDS-PAGE profile, *c* – western blotting with anti-His-tag antibodies

assessed. Among the tested low-molecular-weight ligands the following can be highlighted: terfenadine, a substrate and competitive inhibitor of CYP2J2 (IC_{50} = 8.1 μM) [17], and its metabolite terfenadone (IC_{50} = 0.7 μM) [17]; miconazole suppressing CYP2J2 activity by more than 90 % at 30 μM [3]; 17-ODYA, an inhibitor of CYP-epoxygenases (IC_{50} < 100 nM) [18]; and HET0016, a selective inhibitor of omega-hydroxylases CYP4A/4F (IC_{50} ~9–35 nM) with weaker action on CYP2J2 (IC_{50} ~2.8 μM), allowing a distinction between the omega-hydroxylase and epoxygenase pathways of arachidonic acid metabolism [19].

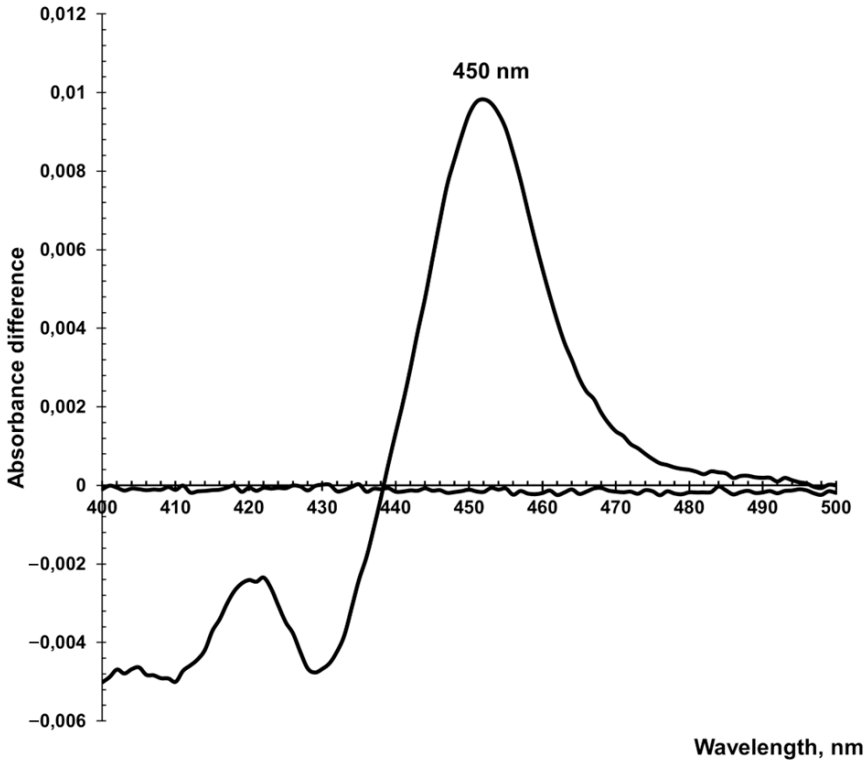
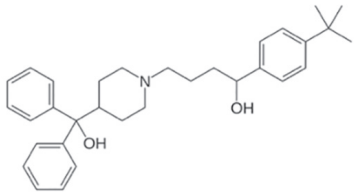
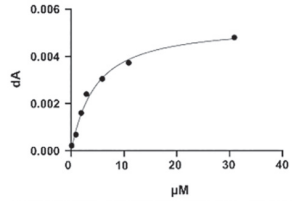
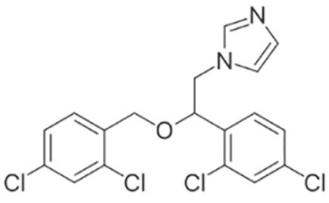
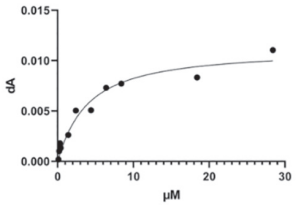
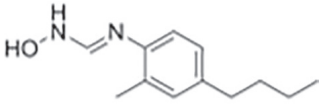
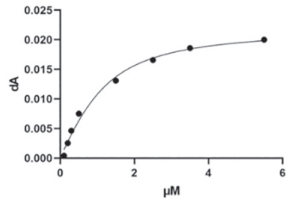
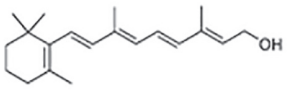
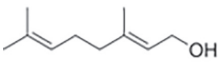
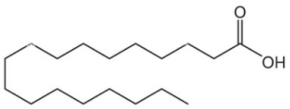
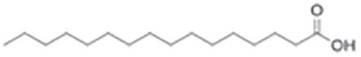
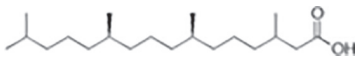
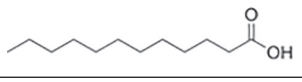


Fig. 3. CO-difference spectrum of recombinant human CYP2J2

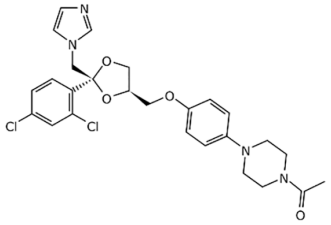
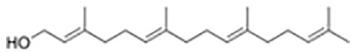
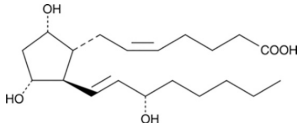
Primary screening was performed by difference spectrophotometry in a microplate format. Upon ligand binding to the active site of cytochrome P450, characteristic changes in the heme absorption spectrum are observed. A Type I spectral response (maximum around 390 nm and minimum around 420 nm) corresponds to binding of substrate-like compounds displacing water molecules from the iron coordination sphere. Type II spectral response (maximum around 430 nm and minimum around 390 nm) is characteristic of azole-type inhibitors coordinating the nitrogen atom directly to the heme iron [20]. Based on primary screening results, compounds with the most pronounced difference signals were selected for subsequent quantitative analysis.

As shown in the graphs, some of the studied compounds demonstrated saturable binding, indicating specific interaction with the active sites of the enzymes. Summary K_d values are presented in Table 1.

Table 1. **Ligand spectrophotometric titration results**

Ligand	Structural formula	Spectral response type	Titration curve	K_d, μM
Terfenadine		I		3.95 ± 0.19
Miconazole		II		3.34 ± 0.17
HET-0016		II		0.54 ± 0.04
Retinol		n/a	n/d	–
Geraniol		n/a	n/d	–
Stearic acid		n/a	n/d	–
Palmitic acid		n/a	n/d	–
Phytanic acid		n/a	n/d	–
Lauric acid		I	n/d	–
17-ODYA		I	n/d	–

End of tabl. 1

Ligand	Structural formula	Spectral response type	Titration curve	K_d, μM
Ketoconazole		n/a	n/d	–
Geranylgeraniol		I	n/d	–
Prostaglandin $F2_a$		I	n/d	–

Note: n/a – no spectral response, n/d – no data. Lauric acid, 17-ODYA, geranylgeraniol, and prostaglandin F2a after the initial assessment of binding (with a distinct spectral response type) in the microplate format failed to show saturable titration curves.

The highest affinity was demonstrated by the inhibitor HET0016, with K_d = 0.54 μM. To validate the experimental system, we compared our measured K_d values with published spectrophotometric binding data for CYP2J2. For terfenadine, our observed K_d of 3.95 μM is in good agreement both with the reported values of 0.90–2.2 μM (Type I binding) determined by spectral titration for wild-type CYP2J2 and its genetic variants [21], and with the K_m value of 1.5 μM for terfenadine hydroxylation in human cardiomyocytes [22]. These binding affinities fall within the range expected for CYP2J2 substrates exhibiting Type I spectral responses. For azole-type inhibitors, direct K_d comparisons from spectrophotometric titration are limited in the literature; published data primarily report functional IC_{50} values from enzymatic inhibition assays, which cannot be directly compared to spectroscopically determined K_d values due to differences in experimental conditions and the influence of substrate competition. The consistency of our terfenadine K_d with published substrate binding constants confirms the reliability of the purification and spectrophotometric characterization methods employed. Several potential Type I ligands, after the initial assessment of binding in the microplate format, failed to show a saturable titration curve (lauric acid, 17-ODYA, geranylgeraniol, and prostaglandin $F2_\alpha$).

Computational screening of potential protein partners of CYP2J2. Prediction confidence was assessed using two complementary metrics implemented in AlphaFold-Multimer. We retained only complexes with an interface predicted TM (iPTM) score ≥ 0.8, indicating high-confidence predicted binding interfaces [12], and a predicted DockQ (pDockQ) score > 0.23, which is a metric calibrated to estimate the structural accuracy of predicted protein–protein complexes [23]. Applying both filters yielded 14 high-confidence predicted interactors for CYP2J2 (Table 2, Figure 4).

Interaction maps were constructed by treating predicted partners as primary nodes and connecting them according to their iPTM scores (Figure 4). To embed these predictions within a broader interactomic context, we queried the STRING database (version 12.0 [24]) for experimentally supported and co-expressed interactions among the predicted partners, generating secondary neighbor nodes. This enrichment strategy revealed a modular organization within the predicted interactome: a STAT3-centric cluster enriched for inflammatory cytokine receptors (IL20RA, IL26, IL22RA1, and IL19), a ubiquitin-ligase module encompassing RNF5, RNF180, and RNF146, and a distinct THAP-domain transcription factor cluster comprising THAP12 and its paralogs (THAP1, THAP3, THAP4, THAP7, and THAP11).

Functional categorization of the predicted interactors reveals that CYP2J2 may participate in a range of cellular processes beyond its canonical monooxygenase activity. The strongest predicted modules involve: (I) ubiquitin-proteasome regulation, through the predicted association with RNF5, RNF180,

Table 2. **Potential protein partners of CYP2J2**

Protein	Localization	Function	Metabolic pathway
EIF3I	Cytoplasm	eIF3 subunit; assembly of the 43S preinitiation complex	Translation initiation
GLUL	Cytoplasm	Glutamine synthetase; synthesizes glutamine from glutamate and NH_4^+	Amino acid metabolism; ammonia detoxification
LONRF1	ER, membrane	E3 ubiquitin ligase; quality control of ER proteins	Stress response
MACC1	Nucleus, cytoplasm	Transcription regulator	HGF/MET and MAPK/ERK signaling
PPP1R37	Nucleus, cytoplasm	Phosphatase regulatory subunit PP1	Protein dephosphorylation
RNF146	Nucleus, cytoplasm	PAR-dependent ubiquitination	DNA repair
RNF180	Membrane, cytoplasm	E3 ubiquitin ligase	Ubiquitin-proteasome pathway
RNF5	ER, mitochondrion	E3 ubiquitin ligase	Apoptosis
SORCS3	Cell membrane, endosomes	Vps10/sortilin receptor	Neurotrophin signaling
STAT3	Nucleus, cytoplasm	Transcription factor; activated by JAK upon cytokine stimulation	JAK/STAT; IL-6/IFN-γ signaling; immune response
TBC1D19	Cytoplasm	Putative Rab-GAP	GTPase regulation
TBCEL	Cytoplasm	Tubule-like protein; regulation of microtubule dynamics	Cytoskeletal organization
THAP12	Nucleus	THAP family transcription factor	Transcription regulation
UNC5A	Cell membrane	Netrin receptor	Netrin-1/UNC5 pathway; axonal navigation

Note: predictions were filtered by iPTM ≥ 0,8 and pDockQ > 0,23. The network topology shown in Figure 4 includes secondary interaction partners retrieved from STRING v12.0 [24] to contextualize predicted interactors within established protein–protein interaction databases.

and RNF146, suggesting a role in proteasome substrate turnover and protein homeostasis; (II) signal transduction, centered on STAT3, which is a transcription factor implicated in various oncogenic processes [25]; (III) translation control, via the predicted interaction with EIF3I, a core component of the eukaryotic translation initiation factor 3 complex; and (IV) transcriptional regulation, through THAP12 and the UNC5A/NTN4 axis.

These predictions should be interpreted with appropriate caution. AlphaFold-Multimer excels at recognizing structurally plausible interfaces but cannot account for cellular concentration gradients, post-translational modifications, or competitive binding dynamics, all of which critically influence true physiological interactions [12]. Moreover, the iPTM and pDockQ thresholds employed here represent heuristic filters optimized for recall in a broad interactome screen and were not validated against a gold-standard CYP2J2 interactome. CYP2J2 has been independently shown to promote the neoplastic phenotype of carcinoma cells [25] and is increasingly recognized as a contributor to diverse pathophysiological processes [26], making the identification of its protein partners of particular interest. Nevertheless, definitive assignment requires experimental validation. We propose proximity-labeling strategies – either TurboID- or APEX2-mediated biotin labeling coupled with mass spectrometry [27, 28] – as the most direct means of confirming these predicted interactions in native cellular contexts. The obtained results

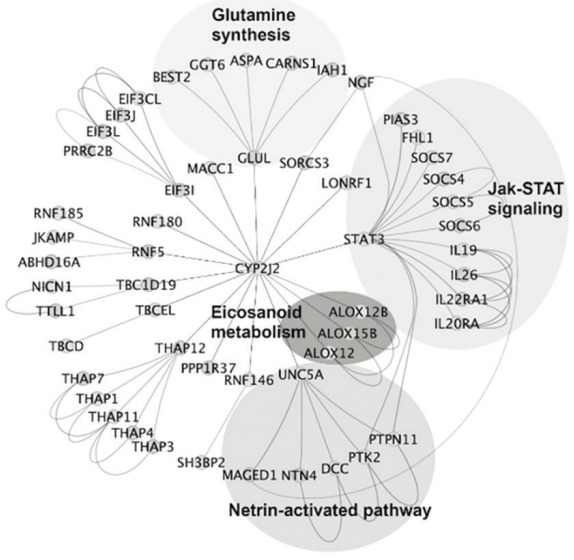


Fig. 4. Protein-protein interaction maps calculated *in silico* (primary interaction nodes are supplemented by secondary nodes)

form an informed list of priority candidates for experimental verification and indicate a possible multifunctional role of CYP2J2 in the cell, which is not limited to xenobiotic metabolism.

Conclusion. In this study, an optimized two-stage procedure for the isolation and purification of recombinant human CYP2J2 was developed, providing the production of high-purity preparations in a native catalytically active form suitable for subsequent biochemical studies and *in vitro* ligand testing. The yield of 21.5 mg/L of culture for CYP2J2 makes the developed system practically applicable for further research.

Functional characterization confirmed that the purified CYP2J2 retained native ligand-binding activity and adequately reproduced affinities known from the literature. The developed system of separation and functional testing creates a reliable basis for further screening of new compounds.

The application of the AlphaPulldown computational approach enabled the identification of 14 potential protein partners of CYP2J2, revealing an unexpected involvement of the enzyme in cellular processes beyond classical monooxygenase metabolism, including the regulation of ubiquitin-proteasome degradation, signal transduction and DNA repair. These findings suggest that CYP2J2 may play a multifunctional role in the cell, and form an informed list of priority candidates for experimental validation by proximity labeling methods.

Acknowledgements. The authors thank the staff of the Institute of Bioorganic Chemistry of the National Academy of Sciences of Belarus for their assistance in performing the experiments. The study was financially supported by the State Committee on Science and Technology of the Republic of Belarus (grant X26SRBG-002).

Благодарности. Авторы выражают благодарность сотрудникам Института биоорганической химии НАН Беларуси за помощь в проведении экспериментов. Исследование было финансово поддержано Государственным комитетом по науке и технологиям Республики Беларусь (грант X26SRBG-002).

References

1. Ma H., Ning J., Ge G., Yang L., Hao D. Research progress of human cytochrome P450 2J2 and its ligands. *Yaoxue Xuebao*, 2017, vol. 52, iss. 1, pp. 26–33 (in Chinese).

2. Enayetallah A. E., French R. A., Grant D. F. Distribution of soluble epoxide hydrolase, cytochrome P450 2C8, 2C9 and 2J2 in human malignant neoplasms. *Journal of Molecular Histology*, 2006, vol. 37, iss. 3–4, pp. 133–141. https://doi.org/10.1007/s10735-006-9050-9

3. Solanki M., Pointon A., Jones B., Herbert K. Cytochrome P450 2J2: Potential Role in Drug Metabolism and Cardiotoxicity. *Drug Metabolism and Disposition*, 2018, vol. 46, iss. 8, pp. 1053–1065. https://doi.org/10.1124/dmd.117.078964

4. Yang B., Graham L., Dikalov S., Mason R. P., Falck J. R., Liao J. K., Zeldin D. C. Overexpression of cytochrome P450 CYP2J2 protects against hypoxia-reoxygenation injury in cultured bovine aortic endothelial cells. *Molecular Pharmacology*, 2001, vol. 60, iss. 2, pp. 310–320. https://doi.org/10.1124/mol.60.2.310

5. Yu Z., Huse L. M., Adler P., Graham L., Ma J., Zeldin D. C., Kroetz D. L. Increased CYP2J expression and epoxyeicosatrienoic acid formation in spontaneously hypertensive rat kidney. *Molecular Pharmacology*, 2000, vol. 57, iss. 5, pp. 1011–1020. https://doi.org/10.1016/s0026-895x(24)26512-3

6. Node K., Huo Y., Ruan X., Yang B., Spiecker M., Ley K., Zeldin D. C., Liao J. K. Anti-inflammatory Properties of Cytochrome P450 Epoxygenase-Derived Eicosanoids. *Science*, 1999, vol. 285, iss. 5431, pp. 1276–1279. https://doi.org/10.1126/science.285.5431.127

7. Spector A. A., Norris A. W. Action of epoxyeicosatrienoic acids on cellular function. *American Journal of Physiology-Cell Physiology*, 2007, vol. 292, iss. 3, pp. C996–C1012. https://doi.org/10.1152/ajpcell.00402.2006

8. Fer M., Dréano Y., Lucas D., Corcos L., Salaün J.-P., Berthou F., Amet Y. Metabolism of eicosapentaenoic and docosahexaenoic acids by recombinant human cytochromes P450. *Archives of Biochemistry and Biophysics*, 2008, vol. 471, iss. 2, pp. 116–125. https://doi.org/ 10.1016/j.abb.2008.01.002

9. Zeldin D. C. Epoxygenase Pathways of Arachidonic Acid Metabolism. *Journal of Biological Chemistry*, 2001, vol. 276, iss. 39, pp. 36059–36062. https://doi.org/10.1074/jbc.R100030200

10. Hashizume T., Imaoka S., Mise M., Terauchi Y., Fujii T., Miyazaki H., Kamataki T., Funae Y. Involvement of CYP2J2 and CYP4F12 in the Metabolism of Ebastine in Human Intestinal Microsomes. *The Journal of Pharmacology and Experimental Therapeutics*, 2002, vol. 300, iss. 1, pp. 298–304. https://doi.org/https://doi.org/10.1124/jpet.300.1.298

11. Leow J. W. H., Gu Y., Chan E. C. Y. Investigating the relevance of CYP2J2 inhibition for drugs known to cause intermediate to high risk torsades de pointes. *European Journal of Pharmaceutical Sciences*, 2023, vol. 187, pp. 106475. https://doi.org/10.1016/j.ejps.2023.106475

12. Jumper J., Evans R., Pritzel A., Green T., Figurnov M., Ronneberger O., Tunyasuvunakool K. et al. Highly accurate protein structure prediction with AlphaFold. *Nature*, 2021, vol. 596, iss. 7873, pp. 583–589. https://doi.org/ 10.1038/s41586-021-03819-2

13. Zhu W., Shenoy A., Kundrotas P., Elofsson A. Evaluation of AlphaFold-Multimer prediction on multi-chain protein complexes. *Bioinformatics*, 2023, vol. 39, iss. 7, art. Btad424. https://doi.org/10.1093/bioinformatics/btad424

14. Zelasko S., Palaria A., Das A. Optimizations to achieve high-level expression of cytochrome P450 proteins using Escherichia coli expression systems. *Protein Expression and Purification*, 2013, vol. 92, iss. 1, pp. 77–87. https://doi.org/10.1016/j.pep.2013.07.017

15. Locuson C. W., Hutzler J. M., Tracy T. S. Visible Spectra of Type II Cytochrome P450-Drug Complexes: Evidence that "Incomplete" Heme Coordination Is Common. *Drug Metabolism and Disposition*, 2007, vol. 35, no. 4, pp. 614–622. https://doi.org/10.1124/dmd.106.012609

16. Omura T., Sato R. The carbon monoxide-binding pigment of liver microsomes. I. Evidence for it hemeprotein nature. *Journal of Biological Chemistry*, 1964, vol. 239, № 7, pp. 2370–2378. https://doi.org/10.1016/S0021-9258(20)82244-3

17. Lafite P., Dijols S., Buisson D., Macherey A.-C., Zeldin D. C., Dansette P. M., Mansuy D. Design and synthesis of selective, high-affinity inhibitors of human cytochrome P450 2J2. *Bioorganic & Medicinal Chemistry Letters*, 2006, vol. 16, iss. 10, pp. 2777–2780. https://doi.org/10.1016/j.bmcl.2006.02.004

18. Zou A. P., Ma Y. H., Sui Z. H., de Montellano P. R. O., Clark J. E., Masters B. S., Roman R. J. Effects of 17-octadecynoic acid, a suicide-substrate inhibitor of cytochrome P450 fatty acid omega-hydroxylase, on renal function in rats. *The Journal of Pharmacology and Experimental Therapeutics*, 1994, vol. 268, iss. 1, pp. 474–481. https://doi.org/10.1016/s0022-3565(25)38498-3

19. Wu C. C., Gupta T., Garcia V., Ding Y., Schwartzman M. L. 20-HETE and Blood Pressure Regulation: Clinical Implications. *Cardiology in Review*, 2014, vol. 22, iss. 1, pp. 1–12. https://doi.org/10.1097/CRD.0b013e3182961659

20. Omura T., Sato R. A new cytochrome in liver microsomes. *Journal of Biological Chemistry*, 1962, vol. 237, pp. 1375–1376. https://doi.org/10.1016/0006-3002(56)90128-7

21. Jeong D., Park H.-G., Lim Y.-R., Lee Y., Kim V., Cho M.-A., Kim D. Terfenadine metabolism of human cytochrome P450 2J2 containing genetic variations (G312R, P351L and P115L). *Drug Metabolism and Pharmacokinetics*, 2018, vol. 33, iss. 1, pp. 61–66. https://doi.org/10.1016/j.dmpk.2017.10.004

22. Evangelista E. A., Kaspera R., Mokadam N. A., Jones J. P., Totah R. A. Activity, inhibition, and induction of cytochrome P450 2J2 in adult human primary cardiomyocytes. *Drug Metabolism and Disposition: The Biological Fate of Chemicals*, 2013, vol. 41, iss. 12, pp. 2087–2094. https://doi.org/ 10.1124/dmd.113.053389

23. Bryant P., Pozzati G., Elofsson A. Improved prediction of protein-protein interactions using AlphaFold2. *Nature Communications*, 2022, vol. 13, iss. 1, art. 1265. https://doi.org/10.1038/s41467-022-28865-w

24. Szklarczyk D., Kirsch R., Koutrouli M., Nastou K., Mehryary F., Hachilif R., Gable A. L. et al. The STRING database in 2023: protein-protein association networks and functional enrichment analyses for any sequenced genome of interest. *Nucleic Acids Research*, 2023, vol. 51, iss. D1, pp. D638–D646. https://doi.org/10.1093/nar/gkac1000

25. Jiang J.-G., Chen C.-L., Card J. W., Yang S., Chen J.-X., Fu X.-N., Ning Y.-G., Xiao X., Zeldin D. C., Wang D. W. Cytochrome P450 2J2 promotes the neoplastic phenotype of carcinoma cells and is up-regulated in human tumors. *Cancer Research*, 2005, vol. 65, iss. 11, pp. 4707–4715. https://doi.org/10.1158/0008-5472.CAN-04-4173

26. Leow J. W. H., Chan E. C. Y. CYP2J2-mediated metabolism of arachidonic acid in heart: A review of its kinetics, inhibition and role in heart rhythm control. *Pharmacology & Therapeutics*, 2024, vol. 258, pp. 108637. https://doi.org/10.1016/j.pharmthera.2024.108637

27. Hung V., Udeshi N. D., Lam S. S., Loh K. H., Cox K. J., Pedram K., Carr S. A., Ting A. Y. Spatially resolved proteomic mapping in living cells with the engineered peroxidase APEX2. *Nature Protocols*, 2016, vol. 11, iss. 3, pp. 456–475. https://doi.org/10.1038/nprot.2016.018

28. Cho K. F., Branon T. C., Udeshi N. D. Proximity labeling in mammalian cells with TurboID and split-TurboID. *Nature Protocols*, 2020, vol. 15, iss. 12, pp. 3971–3999. https://doi.org/10.1038/s41596-020-0399-0

Информация об авторах

Хюппенен Евгения Дмитриевна – младший научный сотрудник. Институт биоорганической химии НАН Беларуси (ул. Академика В. Ф. Купревича, 5/2, 220084, Минск, Республика Беларусь). E-mail: khuppenenevgeniya@gmail.com

Савич Анна Сергеевна – практикант. Институт биоорганической химии НАН Беларуси (ул. Академика В. Ф. Купревича, 5/2, 220084, Минск, Республика Беларусь). E-mail: an.sav1298@gmail.com

Кисель Мария Сергеевна – научный сотрудник. Институт биоорганической химии НАН Беларуси (ул. Академика В. Ф. Купревича, 5/2, 220084, Минск, Республика Беларусь). E-mail: marusen.kee@gmail.com

Свирид Андрей Васильевич – кандидат химических наук, доцент, старший научный сотрудник. Институт биоорганической химии НАН Беларуси (ул. Академика В. Ф. Купревича, 5/2, 220084, Минск, Республика Беларусь). E-mail: svirid@iboch.by

Information about the authors

Khyuppenen Yauhenia D. – Junior Researcher. Institute of Bioorganic Chemistry of the National Academy of Sciences of Belarus (5/2, Academician V. F. Kuprevich Str., 220084, Minsk, Republic of Belarus). E-mail: khuppenenevgeniya@gmail.com

Savich Anna S. – Trainee. Institute of Bioorganic Chemistry of the National Academy of Sciences of Belarus (5/2, Academician V. F. Kuprevich Str., 220084, Minsk, Republic of Belarus). E-mail: an.sav1298@gmail.com

Kisel Mariya S. – Researcher. Institute of Bioorganic Chemistry of the National Academy of Sciences of Belarus (5/2, Academician V. F. Kuprevich Str., 220084, Minsk, Republic of Belarus). E-mail: marusen.kee@gmail.com

Svirid Andrey V. – Ph. D. (Chemistry), Associate Professor, Senior Researcher. Institute of Bioorganic Chemistry of the National Academy of Sciences of Belarus (5/2, Academician V. F. Kuprevich Str., 220084, Minsk, Republic of Belarus). E-mail: svirid@iboch.by